

An exchange-correlation energy for a two-dimensional electron gas in a magnetic field

Rodney Price and S. Das Sarma

Dept. of Physics, University of Maryland, College Park MD 20742

Abstract

We present the results of a variational Monte Carlo calculation of the exchange-correlation energy for a spin-polarized two-dimensional electron gas in a perpendicular magnetic field. These energies are a necessary input to the recently developed current-density functional theory. Landau-level mixing is included in a variational manner, which gives the energy at finite density at finite field, in contrast to previous approaches. Results are presented for the exchange-correlation energy and excited-state gap at $\nu = 1/7, 1/5, 1/3, 1,$ and 2 . We parameterize the results as a function of r_s and ν in a form convenient for current-density functional calculations.

I. INTRODUCTION

Two-dimensional electron systems have been a subject of great interest for some time now, as fascinating phenomena such as the fractional quantum Hall effect and the Wigner solid have been studied intensively. More recently, technological progress has allowed experimenters to fabricate extremely small structures, quantum dots, wires, and so on, that function as external potentials imposed on the 2-D electron gas. An extension of density functional theory, current density functional theory (CDFT) [1,2], has been used to study these phenomena [3,4]. The use of CDFT in this context is attractive, but the calculations to date have been hampered by the lack of an accurate exchange-correlation energy. The ones in use have relied on an interpolation between results at zero magnetic field as a function of density [7,8], and at infinite magnetic field and infinite density [9]; i.e. the lowest Landau level approximation. The CDFT uses derivatives of the exchange-correlation energy with respect to density and magnetic field, so these interpolations will reflect only zero- and infinite- magnetic field and density properties of the system. In addition, since the lowest Landau level approximation requires that the density n and magnetic field B go to infinity with the ratio \sqrt{n}/B held constant, a degree of freedom in the theory is lost.

In this paper, we report the results of variational quantum Monte Carlo calculations of ground-state energies at various integer and fractional magnetic filling factors ν . Our results include an estimate of Landau-level mixing, which allows us to calculate these quantities at finite density and magnetic field. In addition, we find the quasielectron-quasihole gaps at fractional filling factors, including the effect of Landau level mixing here as well. Using both these quantities yields a picture of the true exchange-correlation potential near ν at varying density, including the FQHE-induced cusp.

The CDFT generalizes the usual density functional theory by including the coupling of orbital currents to a magnetic field. The functionals in the theory depend not only on the particle density $n(\vec{r})$ but on the paramagnetic current density $\vec{j}_p(\vec{r})$ as well. (The physical current density $\vec{j}(\vec{r})$ is obtained using the continuity equation.) Solving the CDFT Kohn-

Sham equations [2] for the single-particle orbitals $\psi(\vec{r})$ then lets us define $n(\vec{r})$ and $\vec{j}_p(\vec{r})$ self-consistently,

$$n(\vec{r}) = \sum_i |\psi_i(\vec{r})|^2 \quad (1)$$

$$\vec{j}_p(\vec{r}) = \frac{-i\hbar}{2m} \sum_i [\psi_i^*(\vec{r}) \nabla \psi_i(\vec{r}) - \psi_i(\vec{r}) \nabla \psi_i^*(\vec{r})]. \quad (2)$$

The Kohn-Sham equations involve two exchange-correlation potentials: a scalar potential $V_{xc}(\vec{r})$ and a vector potential $\vec{A}_{xc}(\vec{r})$. These potentials, in turn, are functionals of the exchange-correlation energy E_{xc} as follows,

$$V_{xc}(\vec{r}) = \frac{\delta E_{xc}[n(\vec{r}), \vec{v}(\vec{r})]}{\delta n(\vec{r})} \quad (3)$$

$$\vec{A}_{xc}(\vec{r}) = -\frac{c}{n(\vec{r})} \nabla \times \left(\frac{\delta E_{xc}[n(\vec{r}), \vec{v}(\vec{r})]}{\delta \vec{v}(\vec{r})} \right), \quad (4)$$

where we have defined the vorticity

$$\vec{v}(\vec{r}) = \nabla \times \left(\frac{\vec{j}_p(\vec{r})}{n(\vec{r})} \right). \quad (5)$$

The fact that $\vec{j}_p(\vec{r})$ enters in only through the vorticity $\vec{v}(\vec{r})$ ensures that the potentials are gauge-invariant. In addition, a local current density approximation (LCDA) can be defined in terms of the density $n(\vec{r})$ and the vorticity $\vec{v}(\vec{r})$:

$$E_{xc}[n(\vec{r}), \vec{v}(\vec{r})] = \int d^2r n(\vec{r}) \varepsilon_{xc}(n(\vec{r}), \vec{v}(\vec{r})). \quad (6)$$

As with the LDA, this local energy ε_{xc} is the exchange-correlation energy of a uniform state, in this case the FQHE liquid state. Because the magnetic field in this state is uniform, translational invariance requires that the physical current density $\vec{j}(\vec{r})$ must be uniform and therefore zero. Then

$$\vec{j}(\vec{r}) = \vec{j}_p(\vec{r}) - \frac{en_0}{mc} \vec{A}(\vec{r}) = 0, \quad (7)$$

where $\vec{A}(\vec{r})$ is the physical vector potential and n_0 is the density. Taking the curl of both sides yields

$$\nabla \times \left(\frac{\vec{j}_p(\vec{r})}{n_0} \right) = \frac{e}{mc} \nabla \times \vec{A}(\vec{r}) = \frac{e}{mc} \vec{B}. \quad (8)$$

The left-hand side of (8) is just the vorticity, so using the definition of the magnetic filling factor $\nu = 2\pi n_0 \hbar c / eB$, we have

$$\vec{v}(\vec{r}) = \frac{2\pi \hbar n_0}{m\nu}. \quad (9)$$

The vorticity in the uniform liquid state is then a function of the density n_0 and filling factor ν . Then in order to use the LCDA, we need only find the exchange-correlation energy of the uniform system

$$\bar{\varepsilon}_{xc}(r_s, \nu) = \varepsilon_{xc}(n(\vec{r}), \vec{v}(\vec{r})) \quad (10)$$

as a function of density (or equivalently ion-disk radius $r_s = (\pi n_0)^{-1/2}$) and filling factor ν .

II. VARIATIONAL MONTE CARLO METHOD

We calculate the exchange-correlation energy $\bar{\varepsilon}_{xc}$ using a variational quantum Monte Carlo method. The method uses the Metropolis algorithm to evaluate the energy of a given wavefunction at various values of a variational parameter α . Since we are interested in including Landau-level mixing in the wavefunction only at certain fixed values of ν , where the liquid state is incompressible, we would like to use wavefunctions with suitable correlations built in already. The parameter α will be used to vary the amount of Landau-level mixing in the wavefunction. We can do this if we use lowest Landau level (LLL) wavefunctions for the incompressible states which are well-known: i.e. the Laughlin states for fractional ν or Slater determinants for integer ν . We obtain our variational wavefunction ψ_α by multiplying the LLL wavefunction by a Jastrow factor J_α which lifts the wavefunction partially out of the LLL:

$$J_\alpha = \exp \left[-\alpha \sum_{i < j} u(R_{ij}) \right], \quad (11)$$

where R_{ij} is the distance between the electrons i and j , and $u(r)$ is the so-called pseudopotential.

Now, since $\psi_\alpha = \psi_0 J_\alpha$, where ψ_0 is the LLL wavefunction, varying α varies the amount of Landau-level mixing. (The Jastrow factor forces ψ_α out of the LLL since it is non-analytic.) When $\alpha = 0$ we recover the LLL wavefunction.

The pseudopotential $u(r)$ is chosen to reproduce the zero-point motion of the plasmon modes in two dimensions [8]; then

$$u(r) \sim \frac{1}{\sqrt{r}} \quad (12)$$

at large r . This pseudopotential has a singularity at the origin. In order to minimize the kinetic energy of the wavefunction we should require $u(r) \rightarrow 1/\sqrt{F}$ and $\frac{du}{dr} \rightarrow -\frac{1}{3} \left(\frac{1}{F}\right)^{3/2}$ as $r \rightarrow 0$, where F is another variational parameter. A pseudopotential satisfying these constraints is given by

$$u(r) = \frac{1}{\sqrt{r}} \left[1 - \exp\left(-\sqrt{\frac{r}{F}} - \frac{r}{2F}\right) \right]. \quad (13)$$

In practice, we have found that choosing $F \approx 0.5$ such that $\frac{du}{dr} \rightarrow -\frac{1}{3} \left(\frac{1}{F}\right)^{3/2} = -1$ minimizes the energy at arbitrary α , and thus r_s , quite well. In all the calculations that follow, we have used $F = 0.5$, and varied only the parameter α . A comparison of pseudopotentials (12) and (13) is shown in Figure 1.

Whether our variational wavefunction is the ground state or an excited state, we wish to find its total energy

$$\begin{aligned} E_\alpha &= \langle \alpha | H | \alpha \rangle \\ &= \frac{1}{r_s^2} \langle \alpha | K | \alpha \rangle + \frac{2}{r_s} \langle \alpha | V | \alpha \rangle, \end{aligned} \quad (14)$$

where H is the Hamiltonian, K is the kinetic energy operator, V is the potential energy operator and $|\alpha\rangle$ is the many-particle state. The ion-disk radius r_s factors completely out of both kinetic and potential parts. These two energies, $\langle \alpha | K | \alpha \rangle$ and $\langle \alpha | V | \alpha \rangle$, are computed for a range of α . The energy $E(r_s)$ is found at any given r_s by minimizing E_α with respect

to α . This allows us to find $E(r_s)$ in a corresponding range of r_s without recomputing E_α for each new r_s .

The potential energy $\langle \alpha | V | \alpha \rangle$ is easy to calculate by Monte Carlo. We write

$$\langle \alpha | V | \alpha \rangle = \int d\Omega |\psi_\alpha|^2 V(\Omega) \quad (15)$$

where $\Omega \equiv \{\Omega_1, \dots, \Omega_N\}$ and Ω_i is the position of the i th electron on the sphere. The integral is taken over all Ω_i . We sample from the probability density $|\psi_\alpha|^2$ and sum the potential energy

$$V(\Omega) = \sum_{i < j}^N \frac{1}{R_{ij}}. \quad (16)$$

The kinetic energy sum is also straightforward, but more computationally demanding. The integral becomes

$$\langle \alpha | K | \alpha \rangle = \int d\Omega |\psi_\alpha|^2 \frac{K\psi_\alpha}{\psi_\alpha}. \quad (17)$$

As ψ_α will sometimes involve a projection of an already complex wavefunction to the LLL, we will have to take pains to make this computation efficient. If the projection is necessary, the cost of computing $(K\psi_\alpha)/\psi_\alpha$ is of order N^3 , the most computationally expensive part of the code.

A. Single-particle states and operators

Our calculations are done on the sphere [11] rather than in the plane, as there are no boundaries and the calculations are more efficient. Since the calculations involve Landau-level mixing, which makes the particle density finite, we choose the radius of the sphere $R = \sqrt{N}/2$, where N is the number of particles, to keep the area per particle constant. The magnetic monopole at the center of the sphere has magnetic charge S . We use units of length $a = (\pi n_0)^{-1/2}$ and units of energy $e^2/\epsilon a_B$, where $a_B = \hbar^2 \epsilon / m^* e^2$ and $r_s = a/a_B$. The position of an electron on the sphere is described in spinor coordinates $\chi = (u, v)$, where

$$\begin{pmatrix} u \\ v \end{pmatrix} = \begin{pmatrix} e^{-i\phi/2} \cos \frac{\theta}{2} \\ e^{i\phi/2} \sin \frac{\theta}{2} \end{pmatrix} \quad (18)$$

and (θ, ϕ) is the electron position in spherical coordinates.

The kinetic energy of a single particle on the sphere can be described in terms of its angular momentum [10,11]

$$K = \frac{L^2 - S^2}{R^2}. \quad (19)$$

If we choose the gauge

$$\vec{A} = -\frac{S}{R} \cot \theta \hat{\phi}, \quad (20)$$

we find that the single-particle states are the monopole harmonics [12]

$$\begin{aligned} Y_{S,l,m} &= M_{S,l,m} u^{S-m} v^{S+m} P_{l-s}^{S+m, S-m}(u\bar{u} - v\bar{v}), \\ M_{S,l,m} &= \left[\frac{2l+1}{4\pi} \frac{(l-S)!(l+S)!}{(l-m)!(l+m)!} \right]^{1/2}. \end{aligned} \quad (21)$$

Here $l \geq S$ is the Landau-level index, and $P_n^{\alpha,\beta}(x)$ is a Jacobi polynomial. (A bar over a variable denotes conjugation.) If we set $l = S$ we recover the LLL states given in [11].

The angular momentum operators given in [11] are valid only in the LLL. Operators valid for all Landau levels must include the conjugate variables \bar{u} and \bar{v} . The angular momentum operators then become

$$\begin{aligned} L_+ &= u \frac{\partial}{\partial v} - \bar{v} \frac{\partial}{\partial \bar{u}} \\ L_- &= v \frac{\partial}{\partial u} - \bar{u} \frac{\partial}{\partial \bar{v}} \\ L_z &= \frac{1}{2} \left(-u \frac{\partial}{\partial u} + v \frac{\partial}{\partial v} + \bar{u} \frac{\partial}{\partial \bar{u}} - \bar{v} \frac{\partial}{\partial \bar{v}} \right). \end{aligned} \quad (22)$$

These operators acting on the single-particle states $Y_{S,l,m}$ behave in the expected fashion; that is, L_+ raises m by one, L_- lowers m by one, and L_z has eigenvalue m :

$$\begin{aligned} L_+ Y_{S,l,m} &= \sqrt{(l-m)(l+m+1)} Y_{S,l,m+1} \\ L_- Y_{S,l,m} &= \sqrt{(l+m)(l-m+1)} Y_{S,l,m-1} \\ L_z Y_{S,l,m} &= m Y_{S,l,m}. \end{aligned} \quad (23)$$

Another set of operators exists on the sphere when a magnetic monopole is introduced:

$$\begin{aligned}
T_+ &= -u \frac{\partial}{\partial \bar{v}} + v \frac{\partial}{\partial \bar{u}} \\
T_- &= \bar{u} \frac{\partial}{\partial v} - \bar{v} \frac{\partial}{\partial u} \\
T_z &= \frac{1}{2} \left(u \frac{\partial}{\partial u} + v \frac{\partial}{\partial v} - \bar{u} \frac{\partial}{\partial \bar{u}} - \bar{v} \frac{\partial}{\partial \bar{v}} \right).
\end{aligned} \tag{24}$$

These operators obey the commutation relations for angular momentum (SU(2)) just as the L operators do; i.e. $[T_i, T_j] = \epsilon_{ijk} T_k$. They commute with the L operators: $[\vec{L}, \vec{T}] = 0$, where $\vec{L} = (L_x, L_y, L_z)$, $\vec{T} = (T_x, T_y, T_z)$. Rather than changing the angular momentum quantum number m , however, they change the monopole charge S ,

$$\begin{aligned}
T_+ Y_{S,l,m} &= \sqrt{(l-S)(l+S+1)} Y_{S+1,l,m} \\
T_- Y_{S,l,m} &= \sqrt{(l+S)(l-S+1)} Y_{S-1,l,m} \\
T_z Y_{S,l,m} &= S Y_{S,l,m}.
\end{aligned} \tag{25}$$

Note that $T_z = \hat{\Omega} \cdot \vec{L}$, where $\hat{\Omega}$ is a unit vector indicating a position on the sphere.

Because the monopole harmonics $Y_{S,l,m}$ form a complete basis for a fixed S , any wavefunction ψ which describes a particle moving on the sphere in the presence of a magnetic monopole of charge S must satisfy

$$T_z \psi = S \psi. \tag{26}$$

Now we can calculate the kinetic energy K in (19) more efficiently using the T operators. We use the facts that $T^2 = L^2$ and $[T_+, T_-] = 2T_z$ to get

$$\begin{aligned}
L^2 = T^2 &= \frac{1}{2} (T_- T_+ + T_+ T_-) + T_z^2 \\
&= T_- T_+ + T_z^2 + T_z \\
&= T_- T_+ + S^2 + S.
\end{aligned} \tag{27}$$

Then the kinetic energy operator becomes

$$K = \frac{T_- T_+ + S}{R^2}, \tag{28}$$

and T_-T_+ acting on a wavefunction ψ is enough to give us the kinetic energy. A wavefunction entirely in the LLL has $T_-T_+\psi_0 = 0$.

These two sets of operators are analogous to the inter-Landau level operators a, a^\dagger and intra-Landau level operators b, b^\dagger in the planar geometry. This is easily seen by comparing the effects of these operators on the single-particle states in the plane to the T_\mp and L_\mp operators acting on $Y_{S,l,m}$ on the sphere.

B. Integer quantum Hall states

The integer quantum Hall effect (IQHE) wavefunctions are commonly written as a Slater determinant in which all single-particle states up to the ν^{th} Landau level are filled. Any excitation of this state must involve raising one or more particles up one Landau level, producing an energy gap in the spectrum. This energy gap causes the many-particle state to be incompressible and creates the quantum Hall effect. There is no Landau-level mixing in this wavefunction, since each Landau level is either completely filled or completely empty. This wavefunction is strictly valid only at infinite magnetic field and infinite density. We introduce Landau-level mixing, and thus find the dependence of the total energy on the density, by attaching a Jastrow factor

$$\psi_\alpha = DJ_\alpha, \tag{29}$$

where D is the Slater determinant. The Landau-level mixing costs some kinetic energy but the cost is more than offset by a gain in potential energy, as correlations in the Jastrow factor allow the electrons to stay farther apart.

The ground state is a uniform liquid, but excited states will create regions of charge excess and charge deficit. In order to create a free electron and hole in the excited state, we move these regions of charge excess and deficit as far apart as possible. On the sphere, this is best done by keeping the hole near the north pole and the electron near the south pole. We do this by removing an electron from the $Y_{S,l,-l}$ state and placing it in the $Y_{S,l+1,l+1}$ state

in the first empty Landau level. The remaining interaction between hole and electron is removed by subtracting from the potential energy the interaction between an electron fixed at the south pole and a hole fixed at the north pole.

The Monte Carlo algorithm proceeds by moving a single particle, chosen at random, then calculating the ratio of the new probability density $|\psi'_\alpha|^2$ to the old $|\psi_\alpha|^2$. (Primes on a symbol indicate that it has been computed after the move.) If the new configuration Ω' is more likely than the old Ω , then the move is always accepted; if it is less likely, the move is accepted with probability

$$\frac{|\psi'_\alpha|^2}{|\psi_\alpha|^2} = \frac{D'^2 J'_\alpha{}^2}{D^2 J_\alpha{}^2}. \quad (30)$$

Because the Jastrow factor is a pair product, the computational cost of an update after a single move is of order N . At first glance, the cost of an update to the Slater determinant is also of order N , since we can write

$$D' = \sum_m \phi_m(\Omega'_n) \tilde{D}_{mn}, \quad (31)$$

where we have moved the n^{th} particle, $\phi_m(\Omega'_n)$ is the m^{th} single-particle state after the move, and \tilde{D}_{mn} is the appropriate cofactor. If the move is rejected, we need do no more computation. However, if the move is accepted, we now have to update all the cofactors with index n .

Fahy *et al* [13], and earlier Ceperley *et al* [14] have given an algorithm which computes these cofactors at a cost of order N^2 . They begin the calculation by computing the inverse of the transposed Slater matrix, which gives the cofactors divided by the determinant

$$\bar{D}_{jk} = \frac{\tilde{D}_{jk}}{D}. \quad (32)$$

The ratio of the new determinant to the old is

$$q = \frac{D'}{D} = \sum_m \phi_m(\Omega'_n) \bar{D}_{mn}. \quad (33)$$

The cofactors \tilde{D}_{jk} are never calculated explicitly – they are kept in memory as the elements of the matrix \bar{D}_{jk} . These numbers are updated according to

$$\bar{D}'_{jk} = \begin{cases} \bar{D}_{jk}/q & k = n \\ \bar{D}_{jk} - \frac{\bar{D}_{jn}}{q} \sum_m \phi_m(\Omega'_n) \bar{D}_{mk} & k \neq n. \end{cases} \quad (34)$$

Computing the potential energy is now straightforward using (16).

The kinetic energy is computed by applying $\sum_i T_i^- T_i^+$ to ψ_α and using (28). Because the T_n^\pm are first-order differential operators, both the product rule and the chain rule apply, and we find

$$\begin{aligned} \frac{\sum_i T_i^- T_i^+ \psi_\alpha}{\psi_\alpha} &= \frac{1}{DJ_\alpha} \sum_i T_i^- T_i^+ (DJ_\alpha) \\ &= \sum_i \left[\frac{T_i^- J_\alpha}{J_\alpha} \frac{T_i^+ D}{D} + \frac{T_i^- T_i^+ D}{D} \right. \\ &\quad \left. + \frac{T_i^- D}{D} \frac{T_i^+ J_\alpha}{J_\alpha} + \frac{T_i^- T_i^+ J_\alpha}{J_\alpha} \right]. \end{aligned} \quad (35)$$

The action of T_n^\pm on the determinant is easily found,

$$\frac{T_n^\pm D}{D} = \sum_m T_n^\pm \phi_m(\Omega_n) \bar{D}_{mn} \quad (36)$$

$$\frac{T_n^- T_n^+ D}{D} = \sum_m T_n^- T_n^+ \phi_m(\Omega_n) \bar{D}_{mn} \quad (37)$$

The second quantity (37), when summed over all n , is just the excess kinetic energy of the determinant D , a constant independent of the electron positions. The first quantity (36) can be also be computed quickly, since the single-particle states are the monopole harmonics $Y_{S,l,m}(\Omega_n)$, and we have already computed the matrix elements \bar{D}_{nm} .

The action of T_n^\pm on the Jastrow factor is found most conveniently by defining two rotationally-invariant quantities on the sphere,

$$r_{ij} \equiv u_i v_j - v_i u_j \quad (38)$$

$$s_{ij} \equiv \bar{u}_i u_j + \bar{v}_i v_j. \quad (39)$$

Here $|r_{ij}|$ is proportional to the chord distance on the sphere between particles i and j , and s_{ij} is related to the particle's center of mass. Their property of rotational invariance is verified by applying an arbitrary rotation

$$\begin{pmatrix} \bar{u}_0 & \bar{v}_0 \\ -v_0 & u_0 \end{pmatrix} \begin{pmatrix} u \\ v \end{pmatrix} = \begin{pmatrix} \bar{u}_0 u + \bar{v}_0 v \\ u_0 v - v_0 u \end{pmatrix}, \quad (40)$$

substituting for u and v in (38) and (39), and using the identity $u\bar{u} + v\bar{v} = 1$.

The T_n^\pm operators have a particularly simple effect on r_{ij} and s_{ij} ,

$$\begin{aligned} T_i^- r_{ij} &= -s_{ij} & T_i^- \bar{r}_{ij} &= 0 & T_i^- s_{ij} &= 0 & T_i^- \bar{s}_{ij} &= \bar{r}_{ij} \\ T_i^+ r_{ij} &= 0 & T_i^+ \bar{r}_{ij} &= \bar{s}_{ij} & T_i^+ s_{ij} &= -r_{ij} & T_i^+ \bar{s}_{ij} &= 0 \end{aligned} \quad (41)$$

Other identities are found using $r_{ji} = -r_{ij}$ and $s_{ji} = \bar{s}_{ij}$. Then the action of T_i^\pm on the Jastrow factor is

$$\begin{aligned} \frac{T_n^\pm J_\alpha}{J_\alpha} &= \frac{1}{J_\alpha} T_n^\pm \exp \left[-\alpha \sum_{i < j} c(r_{ij} \bar{r}_{ij}) \right] \\ &= -\alpha \sum_i' \left[(T_n^\pm r_{ni}) \bar{r}_{ni} + r_{ni} (T_n^\pm \bar{r}_{ni}) \right] c'(r_{ni} \bar{r}_{ni}), \end{aligned} \quad (42)$$

where $c'(x) \equiv \partial c / \partial x$, the prime on the sum indicates that the sum is over all $i \neq n$, and we have defined a new pseudopotential function $c(r^2) \equiv u(r)$ equivalent to the old with a different argument. Applying (41) gives explicit expressions. The quantity $(T_n^- T_n^+ J_\alpha) / J_\alpha$ is evaluated in a similar fashion.

C. Fractional quantum Hall states

It is well-known that the FQHE occurs at certain fractional filling factors ν . In contrast to the IQHE, which is a single-particle phenomenon, the FQHE is caused by interactions between the particles. At these fractional fillings the particles can avoid each other best by staying in high angular momentum states relative to each other. Excitations in this state must have a gap, since any excitation has to lower at least one particle's angular momentum with respect to the others, using a finite amount of energy.

The excitations appear as quasihole-quasielectron pairs, each carrying a fractional charge. The energy required to create the pair, the gap energy E_g , determines the magnitude of the cusp that appears in the ground-state energy with respect to ν , since the states just off the

FQHE filling factors ν must have a finite number of quasiparticles. The magnitude of the cusp is related to the gap [15] by

$$E_g = \nu^2 \left[\frac{\partial E}{\partial \nu} \Big|_{\nu=\nu+} - \frac{\partial E}{\partial \nu} \Big|_{\nu=\nu-} \right] \quad (43)$$

In this paper we will consider only the principal states at $\nu = 1/(p+1)$, p even. The Laughlin wavefunctions ψ_L describing the states on the sphere [10] are written $\psi_L = L^{p+1}$ where

$$L \equiv \prod_{i < j} (u_i v_j - v_i u_j). \quad (44)$$

We need an explicit wavefunction for the quasihole-quasielectron state as well. In order to do so we turn to the composite fermion picture, where

$$\psi_{CF} = DL^p. \quad (45)$$

Here the Slater determinant D is a full Landau level when describing the principal states. Since at this filling D is a Van der Monde determinant, $D = L$ and the two forms are equivalent.

In the composite fermion picture, however, we think of D as describing the particles, and the remaining factor L^p as attaching p magnetic flux quanta to each particle. To complete the picture we must then project the new wavefunction onto the LLL

$$\psi_{CF}^0 = \mathcal{P} [DL^p], \quad (46)$$

where \mathcal{P} is the projection operator. To excite a quasiparticle pair, we follow the IQHE example by moving an electron in D from the LLL to the second Landau level. We again want the quasiparticles as far apart as possible, so we put the quasihole on the north pole and the quasielectron on the south pole. As before, we do this by moving the electron in $Y_{S,S,-S}$ to $Y_{S,S+1,S+1}$. We then subtract from the potential energy the interaction of fractionally-charged particles on opposite poles to model a free quasihole and quasielectron.

Unfortunately, projecting the composite fermion wavefunction to the LLL is, to the authors' knowledge, an unsolved problem. It has been done for a small (up to 12) number

of particles only by explicitly decomposing the wavefunction in the Slater determinant basis and keeping only those terms in the LLL [16]. There is, however, a trick recently used by Bonesteel [17] which can project a wavefunction with a single electron, or perhaps two or three, in the second Landau level to the LLL. If the occupancy of the second Landau level is at most one, for example, ψ_{CF} can be decomposed as

$$\psi_{CF} = \psi_{CF}^0 + \psi_{CF}^1, \quad (47)$$

where ψ_{CF}^0 is entirely in the LLL, and ψ_{CF}^1 has exactly one electron in the second Landau level. Letting the excess kinetic energy operator $\sum_n T_n^- T_n^+$ act on ψ_{CF} , then

$$\begin{aligned} \sum_n T_n^- T_n^+ \psi_{CF} &= 0 \psi_{CF}^0 + \Delta \psi_{CF}^1 \\ \Rightarrow \left(\sum_n T_n^- T_n^+ - \Delta \right) \psi_{CF} &= -\Delta \psi_{CF}^0 \end{aligned} \quad (48)$$

is all in the LLL. Here $\Delta = 2S + 2$ is the separation between Landau levels, and we have shifted the zero of the kinetic energy to ignore zero-point motion. Remembering the definition in (38), and normalizing by the unprojected wavefunction, we find

$$\begin{aligned} \frac{\psi_{CF}^0}{\psi_{CF}} &= \frac{1}{\psi_{CF}^0 \Delta} \left[\sum_n T_n^- T_n^+ - \Delta \right] (DL^p) \\ &= \frac{p}{\Delta} \sum_n \frac{T_n^- L}{L} \frac{T_n^+ D}{D} + \left(\frac{\Delta_D}{\Delta} - 1 \right) \end{aligned} \quad (49)$$

where we have used the fact that $T_n^+ L = 0$ and

$$\Delta_D D = \sum_n T_n^- T_n^+ D. \quad (50)$$

We have already found $(T_n^+ D)/D$. Writing $L = \prod_{i < j} r_{ij}$ and using (41), we find

$$\frac{T_n^- L}{L} = -\sum_i' \frac{s_{ni}}{r_{ni}}. \quad (51)$$

In order to introduce Landau-level mixing into the wavefunction, we again attach a Jastrow factor

$$\psi_\alpha = \mathcal{P} [DL^p] J_\alpha. \quad (52)$$

The potential energy, as before, can be found by averaging (16) over all configurations generated in the Monte Carlo code by $|\psi_\alpha|^2$.

The kinetic energy for the ground state can be found in a straightforward manner, since the ground-state variational wavefunction is

$$\psi_\alpha = L^{p+1} J_\alpha. \quad (53)$$

To calculate the kinetic energy, we use

$$\begin{aligned} \frac{T_n^- T_n^+ \psi_\alpha}{\psi_\alpha} &= \frac{1}{L^{p+1} J_\alpha} \sum_n T_n^- T_n^+ (L^{p+1} J_\alpha) \\ &= (p+1) \sum_n \frac{T_n^- L}{L} \frac{T_n^+ J_\alpha}{J_\alpha} + \sum_n \frac{T_n^- T_n^+ J_\alpha}{J_\alpha}, \end{aligned} \quad (54)$$

where we have used the fact that $T_n^+ L = 0$. We have previously shown how to compute each of these terms.

Computing the kinetic energy for the quasihole-quasielectron state is more involved, due to the presence of the projection operator \mathcal{P} . The complexity arises from the fact that our implementation of \mathcal{P} involves a product of two T operators, and the kinetic energy uses another product of two T operators. We need to calculate the quantity

$$\frac{\sum_m T_m^- T_m^+ (\psi_{CF}^0 J_\alpha)}{\psi_{CF} J_\alpha} = \sum_m \frac{T_m^- \psi_{CF}^0}{\psi_{CF}} \frac{T_m^+ J_\alpha}{J_\alpha} + \frac{\psi_{CF}^0}{\psi_{CF}} \sum_m \frac{T_m^- T_m^+ J_\alpha}{J_\alpha}. \quad (55)$$

The only term we have not yet found is $(T_m^- \psi_{CF}^0)/\psi_{CF}$. We have

$$\begin{aligned} \frac{T_m^- \psi_{CF}^0}{\psi_{CF}} &= \frac{T_m^- \mathcal{P}[DL^p]}{DL^p} \\ &= \frac{1}{DL^p} T_m^- \left\{ \left[\frac{p}{\Delta} \sum_n \frac{T_n^- L}{L} \frac{T_n^+ D}{D} + \left(\frac{\Delta_D}{\Delta} - 1 \right) \right] DL^p \right\} \\ &= \frac{p(p-1)}{\Delta} \frac{T_m^- L}{L} \sum_n \frac{T_n^- L}{L} \frac{T_n^+ D}{D} + \\ &\quad \frac{p}{\Delta} \sum_n \left[\frac{T_m^- T_n^- L}{L} \frac{T_n^+ D}{D} + \frac{T_n^- L}{L} \frac{T_m^- T_n^+ D}{D} \right] + \\ &\quad \left(\frac{\Delta_D}{\Delta} - 1 \right) \left[\frac{T_m^+ D}{D} + p \frac{T_m^- L}{L} \right]. \end{aligned} \quad (56)$$

The two terms not yet computed are $(T_m^- T_n^- L)/L$ and $(T_m^- T_n^+ D)/D$.

We can find $(T_m^- T_n^- L)/L$ in a straightforward manner, by applying (41) and (51). First we note that

$$T_m^- \left(\frac{s_{ni}}{r_{ni}} \right) = \delta_{mn} \left(\frac{s_{ni}}{r_{ni}} \right)^2 - (1 - \delta_{mn}) \frac{\delta_{mi}}{r_{ni}^2}, \quad (57)$$

where we assume that $n \neq i$ and we use the identity $s_{ij} \bar{s}_{ij} + r_{ij} \bar{r}_{ij} = 1$. Then we have

$$\begin{aligned} \frac{T_m^- T_n^- L}{L} &= \left(\sum_{i, i \neq n} \frac{s_{ni}}{r_{ni}} \right) \left(\sum_{i, i \neq m} \frac{s_{mi}}{r_{mi}} \right) + \\ &\quad \frac{1 - \delta_{mn}}{r_{mn}^2} - \delta_{mn} \sum_{i, i \neq m} \left(\frac{s_{mi}}{r_{mi}} \right)^2. \end{aligned} \quad (58)$$

The first two sums have been computed earlier, and the sum in the last term enters only when $n = m$.

The second term $(T_m^- T_n^+ D)/D$ is computed easily when $m = n$,

$$\frac{T_n^- T_n^+ D}{D} = \sum_i T_n^- T_n^+ \phi_i(\Omega_n) \bar{D}_{in}. \quad (59)$$

When $m \neq n$ we use the identity (derived in the appendix)

$$\begin{aligned} \frac{T_m^- T_n^+ D}{D} &= \left(\sum_i T_n^+ \phi_i(\Omega_n) \bar{D}_{in} \right) \left(\sum_i T_m^- \phi_i(\Omega_m) \bar{D}_{im} \right) - \\ &\quad \left(\sum_i T_n^+ \phi_i(\Omega_n) \bar{D}_{im} \right) \left(\sum_i T_m^- \phi_i(\Omega_m) \bar{D}_{in} \right), \end{aligned} \quad (60)$$

where the $\phi_i(\Omega_j)$ are again the single-particle wavefunctions. The N^3 scaling of the time required to compute the kinetic energy of ψ_{CF}^0 arises from (60), since (60) has to be computed for all N^2 pairs (m, n) and each computation scales as N .

III. IMPLEMENTATION OF MONTE CARLO METHOD

The implementation of the Monte Carlo procedure described above requires some adjustment in practice. The pseudopotential $u(r)$, (13), if put directly on the sphere, will cause wild fluctuations in the kinetic energy calculation. The cause is found in the cusp at $r = 2R$, introduced in the pseudopotential by the mapping to the sphere. In effect, a δ -function in

the second derivative of the trial wavefunction appears if $\partial u/\partial r \neq 0$ at $r = 2R$. We remove the cusp by making a linear combination of $u(r)$'s with different arguments,

$$\tilde{u}(r) = u(r) + u(4R - r). \quad (61)$$

Then

$$\left. \frac{\partial \tilde{u}}{\partial r} \right|_{r=2R} = \left. \frac{\partial u}{\partial r} \right|_{r=2R} - \left. \frac{\partial u}{\partial r} \right|_{4R-r=2R}, \quad (62)$$

$\partial u/\partial r = 0$ at $r = 2R$, and the cusp is removed. The Jastrow factor is now

$$J_\alpha = \exp \left[-\alpha \sum_{i < j} \tilde{u}(|r_{ij}|) \right], \quad (63)$$

where we have used the definition (38). With the variational parameter α appearing only outside the pseudopotential, we can compute potential and kinetic energies for a range of α , then do the minimization with respect to α for any number of values for r_s without repeating the Monte Carlo calculation.

Calculating the IQHE ground-state potential and kinetic energies by the Monte Carlo procedure in section II B is straightforward, since the trial wavefunction is simple. The variance in the result is small and scales as \sqrt{N} . The energy gap to the first excited state is more problematic, however. If we move an electron up to the next Landau level, creating an electron-hole pair, we must evaluate the pair energy by subtracting the ground state total energy from the excited state total energy. The variance in the Monte Carlo results for either state is then of the same order as the energy gap, and the results of the calculation are obscured by the statistical noise. Increasing N only worsens the problem, since the energy gap remains approximately constant with N , but the variance in the energies gets larger.

We circumvent this difficulty in the manner recommended by Ceperley in [19], by sampling from the ground-state wavefunction and computing the excited state energy and ground state energy simultaneously. The two energies are then correlated: an upward fluctuation in the ground state energy always correlates with a nearly equivalent upward fluctuation in the excited state energy, for example, and the variance of the difference is small.

The computation of the excited state energy is implemented in the following way: the ground state energy is calculated in the Monte Carlo code as

$$\begin{aligned}\langle \alpha | H | \alpha \rangle_{\text{gnd}} &= \int d\Omega \left| \psi_{\alpha}^{\text{gnd}} \right|^2 \frac{H \psi_{\alpha}^{\text{gnd}}}{\psi_{\alpha}^{\text{gnd}}} \\ &= \sum_n \frac{H \psi_{\alpha}^{\text{gnd}}}{\psi_{\alpha}^{\text{gnd}}},\end{aligned}\tag{64}$$

since the sample configurations are drawn from $\psi_{\alpha}^{\text{gnd}}(\Omega)$. (As before, we define $\Omega = \{\Omega_1, \dots, \Omega_N\}$, where Ω_i is the position of the i^{th} electron.) We write the excited state energy as

$$\begin{aligned}\langle \alpha | H | \alpha \rangle_{\text{ex}} &= \int d\Omega \left| \psi_{\alpha}^{\text{ex}} \right|^2 \frac{H \psi_{\alpha}^{\text{ex}}}{\psi_{\alpha}^{\text{ex}}} \\ &= \kappa \int d\Omega \left| \psi_{\alpha}^{\text{gnd}} \right|^2 \left| \frac{\psi_{\alpha}^{\text{ex}}}{\psi_{\alpha}^{\text{gnd}}} \right|^2 \frac{H \psi_{\alpha}^{\text{ex}}}{\psi_{\alpha}^{\text{ex}}} \\ &= \kappa \sum_n \left| \frac{\psi_{\alpha}^{\text{ex}}(\Omega_n)}{\psi_{\alpha}^{\text{gnd}}(\Omega_n)} \right|^2 \frac{H \psi_{\alpha}^{\text{ex}}(\Omega_n)}{\psi_{\alpha}^{\text{ex}}(\Omega_n)},\end{aligned}\tag{65}$$

where the normalization κ is no longer 1,

$$\begin{aligned}\kappa^{-1} &= \int d\Omega \left| \psi_{\alpha}^{\text{gnd}} \right|^2 \left| \frac{\psi_{\alpha}^{\text{ex}}}{\psi_{\alpha}^{\text{gnd}}} \right|^2 \\ &= \sum_n \left| \frac{\psi_{\alpha}^{\text{ex}}(\Omega_n)}{\psi_{\alpha}^{\text{gnd}}(\Omega_n)} \right|^2.\end{aligned}\tag{66}$$

Calculating the ground state energy for the FQHE states is comparatively straightforward as well, using (64). The FQHE ground state energies in this paper were all done in this manner. Because of the complexity of the excited state wavefunction, however, it is difficult to follow the recipe in (65). Instead, we sample from the unprojected wavefunction

$$\psi_{\alpha}^{\text{un}} = D L^p J_{\alpha}.\tag{67}$$

We compute both excited state and ground state wavefunctions similarly to (65). Define $\psi_{\alpha}^{\text{gnd}} = \mathcal{P} [D_{\text{gnd}} L^p] J_{\alpha} = L^{p+1} J_{\alpha}$ and $\psi_{\alpha}^{\text{ex}} = \mathcal{P} [D_{\text{ex}} L^p] J_{\alpha}$. For the ground state,

$$\langle \alpha | H | \alpha \rangle_{\text{gnd}} = \int d\Omega \left| \psi_{\alpha}^{\text{gnd}} \right|^2 \frac{H \psi_{\alpha}^{\text{gnd}}}{\psi_{\alpha}^{\text{gnd}}}$$

$$\begin{aligned}
&= \kappa_{\text{gnd}} \int d\Omega |\psi_{\alpha}^{\text{un}}|^2 \left| \frac{\psi_{\alpha}^{\text{gnd}}}{\psi_{\alpha}^{\text{un}}} \right|^2 \frac{H\psi_{\alpha}^{\text{gnd}}}{\psi_{\alpha}^{\text{gnd}}} \\
&= \kappa_{\text{gnd}} \sum_n \left| \frac{\psi_{\alpha}^{\text{gnd}}(\Omega_n)}{\psi_{\alpha}^{\text{un}}(\Omega_n)} \right|^2 \frac{H\psi_{\alpha}^{\text{gnd}}(\Omega_n)}{\psi_{\alpha}^{\text{gnd}}(\Omega_n)},
\end{aligned} \tag{68}$$

and for the excited state

$$\begin{aligned}
\langle \alpha | H | \alpha \rangle_{\text{ex}} &= \int d\Omega |\psi_{\alpha}^{\text{ex}}|^2 \frac{H\psi_{\alpha}^{\text{ex}}}{\psi_{\alpha}^{\text{ex}}} \\
&= \kappa_{\text{ex}} \int d\Omega |\psi_{\alpha}^{\text{un}}|^2 \left| \frac{\psi_{\alpha}^{\text{ex}}}{\psi_{\alpha}^{\text{un}}} \right|^2 \frac{H\psi_{\alpha}^{\text{ex}}}{\psi_{\alpha}^{\text{ex}}} \\
&= \kappa_{\text{ex}} \sum_n \left| \frac{\psi_{\alpha}^{\text{ex}}(\Omega_n)}{\psi_{\alpha}^{\text{un}}(\Omega_n)} \right|^2 \frac{H\psi_{\alpha}^{\text{ex}}(\Omega_n)}{\psi_{\alpha}^{\text{ex}}(\Omega_n)}.
\end{aligned} \tag{69}$$

The normalizations κ_{gnd} and κ_{ex} are calculated in the same way as (66).

We checked the results of this calculation by comparing the ground state energies found using (68) to the ground state energies found using (64). The energies were identical to within the statistical variations.

The initial electron configuration for each Monte Carlo run must be chosen carefully to avoid underflow of the computer's arithmetic. The probability of generating a configuration from the trial wavefunction identical to that made by placing electrons at random on the sphere is so low that the initial calculation of the Slater determinant D will invariably underflow. To work around this problem we use an initial configuration which keeps the particles as far apart as possible. The probability of drawing this configuration from the trial wavefunction is much higher than that of a random configuration, so the initial computation of D will not underflow.

This configuration is generated using some code borrowed from Jon Leech [18]. It begins with six electrons; two on the north and south poles and four evenly distributed around the equator, forming the vertices of an octahedron. Each face is a triangle, which can be subdivided into four smaller triangles, as in Figure 2. Placing electrons at the vertices of these new triangles generates a configuration of 18 electrons. Repeating the process generates another configuration of 66 electrons, and so on. The electrons are, of course, not directly on the vertices of the new triangles, but lie on the surface of the sphere, on a line joining

each triangle vertex to the origin. A few electrons can be removed from this configuration, as needed, without underflowing the computer arithmetic.

IV. RESULTS

We have obtained exchange-correlation energies $\bar{\epsilon}_{\text{xc}}$ and gap energies Δ_{eh} at $\nu = 1/7, 1/5, 1/3, 1,$ and 2 as a function of r_s , using a model [20] of the electron-electron interaction

$$V(r) = \frac{1}{\sqrt{r^2 + \lambda^2}}. \quad (70)$$

Setting $\lambda = 0$ recovers the Coulomb interaction. The softer interactions modeled by (70) more closely approximate the interaction experienced by electrons in a GaAs-AlGaAs heterojunction. We have calculated $\bar{\epsilon}_{\text{xc}}$ and Δ_{eh} for $\lambda = 0, 0.2, 0.5,$ and 1.0 .

Numerical fits for our computed exchange-correlation energies are given in Tables I-IV. The Monte Carlo results are modeled using an order (2,2) rational function fit,

$$\bar{\epsilon}_{\text{xc}} = \frac{a_0 + a_1 r_s + a_2 r_s^2}{1 + b_1 r_s + b_2 r_s^2}. \quad (71)$$

This form ensures that the energy $\bar{\epsilon}_{\text{xc}}$ remains finite as $r_s \rightarrow \infty$. The Monte Carlo code produced good results from $r_s = 0$ to $r_s = 50$ in most cases, although when $\bar{\epsilon}_{\text{xc}}$ changed rapidly, the code gave results only up to $r_s = 35$. This was true only for the Coulomb interaction at $\nu = 1$ and 2 , with fitting parameters given in Table I. A typical set of results is shown in Figure 3.

The uncertainty in the numbers from the Monte Carlo code are given in the tables by showing the standard deviation in the values of the last digit in the parameter a_0 in parentheses. The errors in $\bar{\epsilon}_{\text{xc}}$ for higher λ are much smaller than for the Coulomb case, since for a given change in inter-electron spacing, the softer interactions produce a smaller (sometimes much smaller) change in the total energy of the system. The fluctuations in the instantaneous energy in the Monte Carlo code are then smaller, and the corresponding results more accurate.

Numerical fits for the gap energies Δ_{eh} are given in Tables V-VIII. Here we also use a rational function fit, but since the uncertainty in the gap energies are relatively large we use only an order (1,1) fit,

$$\Delta_{\text{eh}} = \frac{a_0 + a_1 r_s}{1 + b_1 r_s}. \quad (72)$$

Gap energies for $\nu = 1/3$ and $1/7$ are shown in Figures 4 and 5, respectively.

These energies were calculated with an 18-particle system, rather than the 66-particle system used to calculate the exchange-correlation energies. Fluctuations in the larger system tend to overwhelm the gap energy, since only one particle (or composite particle) is involved in creating the excitation whose energy we are measuring.

The quasihole-quasielectron (or in the case of integer ν , hole-electron) interaction between particles of opposite charge on the north and south poles is removed by subtracting the interaction of point charges of appropriate magnitude at the same places. The uncertainty in the results is given, as before, in the numbers in parentheses beside the values for a_0 in Tables V-VIII. We keep three digits in the fitting parameters other than a_0 to remove errors in the fit caused by truncation.

V. SUMMARY

We have calculated exchange-correlation energies and energy gaps between ground state and first excited state for quantum Hall states at various filling factors ν using a model electron-electron interaction which is realistic for electrons in GaAs-AlGaAs heterostructures. Including Landau-level mixing in the calculation allows us to present results at finite magnetic field and electron density. Our results are presented in the form of numerical fits to simple rational functions, convenient for use in current-density functional theory calculations. Calculating energy gaps as well as ground state energies allows us to model the energy near the quantum Hall state realistically. This work has been supported by the ONR and the NSF.

**APPENDIX A: TWO SINGLE-PARTICLE OPERATORS ACTING ON A
SLATER DETERMINANT**

Let the two single-particle operators be \hat{O}_i and \hat{O}_j , where i and j are particle indices and $i \neq j$. We wish to calculate $(\hat{O}_i\hat{O}_jD)/D$ where D is a Slater determinant composed of single-particle states $\phi_i(\Omega_j)$. In the following \tilde{D}_{ij} will be the i, j^{th} cofactor of the Slater matrix. Transposing and taking the inverse of the Slater matrix, we find $\bar{D}_{ij} = \tilde{D}_{ij}/D$. The first operator acting on D gives

$$\hat{O}_jD = \sum_k \hat{O}_j\phi_k(\Omega_j)\tilde{D}_{kj}. \quad (\text{A1})$$

The new object \hat{O}_jD can be thought of as a new Slater determinant D' . The new Slater matrix is identical to the old Slater matrix with the exception of the j^{th} column, which changes from $\phi_m(\Omega_j)$ to $\hat{O}_j\phi_m(\Omega_j)$, $1 \leq m \leq N$. Given the old inverse matrix elements \bar{D}_{ij} , we would like to find the new elements \bar{D}'_{ij} . The Sherman-Morrison formula (equations (2.7.4) and (2.7.5) of [21]) gives

$$\bar{D}'_{ki} = \bar{D}_{ki} - \frac{z_i w_k}{1 + z_j} \quad (\text{A2})$$

where we define (following the notation in [21])

$$\begin{aligned} u_k &= \hat{O}_j\phi_k(\Omega_j) - \phi_k(\Omega_j) \\ v_k &= \delta_{jk} \\ z_k &= \sum_m \bar{D}_{mk}u_m \\ w_k &= \sum_m \bar{D}_{km}v_m = \bar{D}_{kj}. \end{aligned} \quad (\text{A3})$$

Substituting, we find that

$$\begin{aligned} z_j &= \sum_k \hat{O}_j\phi_k(\Omega_j)\bar{D}_{kj} - \sum_k \phi_k(\Omega_j)\bar{D}_{kj} \\ &= \frac{\hat{O}_jD}{D} - 1. \end{aligned} \quad (\text{A4})$$

Now let the second operator \hat{O}_i act on the new Slater determinant

$$\begin{aligned}
\frac{\hat{O}_i D'}{D} &= \frac{1}{D} \sum_k \hat{O}_i \phi_k(\Omega_i) (\bar{D}'_{ki} D') \\
&= \frac{D'}{D} \left[\sum_k \hat{O}_i \phi_k(\Omega_i) \bar{D}_{ki} - \sum_k \hat{O}_i \phi_k(\Omega_i) z_i \bar{D}_{kj} \left(\frac{\hat{O}_j D}{D} \right)^{-1} \right], \tag{A5}
\end{aligned}$$

where we have used (A2) and (A3). Recognizing that $D'/D = (\hat{O}_j D)/D$ and using (A1), we rewrite (A5) as

$$\frac{\hat{O}_i \hat{O}_j D}{D} = \frac{\hat{O}_j D}{D} \frac{\hat{O}_i D}{D} - z_i \sum_k \hat{O}_i \phi_k(\Omega_i) \bar{D}_{kj}. \tag{A6}$$

Here, using (A3) and the fact that \bar{D}_{ki} is an inverse matrix element

$$\begin{aligned}
z_i &= \sum_k \bar{D}_{ki} [\hat{O}_j \phi_k(\Omega_j) - \phi_k(\Omega_j)] \\
&= \sum_k \hat{O}_j \phi_k(\Omega_j) \bar{D}_{ki} - \delta_{ij}, \tag{A7}
\end{aligned}$$

but $i \neq j$ by assumption, so we obtain the result,

$$\begin{aligned}
\frac{\hat{O}_i \hat{O}_j D}{D} &= \left(\sum_k \hat{O}_j \phi_k(\Omega_j) \bar{D}_{kj} \right) \left(\sum_k \hat{O}_i \phi_k(\Omega_i) \bar{D}_{ki} \right) - \\
&\quad \left(\sum_k \hat{O}_j \phi_k(\Omega_j) \bar{D}_{ki} \right) \left(\sum_k \hat{O}_i \phi_k(\Omega_i) \bar{D}_{kj} \right). \tag{A8}
\end{aligned}$$

APPENDIX B: SPLINE INTERPOLATION BETWEEN QHE STATES

Interpolation between energies E_j of adjacent quantum Hall states in filling factor ν can be conveniently accomplished using cubic splines. The energy cusp at each state is included in the interpolation by requiring that the discontinuity in derivative of energy E be given by (43), rather than requiring that it be zero, as normally done. If the filling factor (energy) of the j^{th} state is given as $\nu_j(E_j)$, and the discontinuities in derivative are Δ_j , the equations defining the spline parameters E_j'' , following (3.3.7) of [21], are

$$\frac{\nu_j - \nu_{j-1}}{6} E_{j-1}'' + \frac{\nu_{j+1} - \nu_{j-1}}{3} E_j'' + \frac{\nu_{j+1} - \nu_j}{6} E_{j+1}'' = \frac{E_{j+1} - E_j}{\nu_{j+1} - \nu_j} - \frac{E_j - E_{j-1}}{\nu_j - \nu_{j-1}} + \Delta_j \tag{B1}$$

Solving this system of equations for the E_j'' parameters, and using them following [21] section 3.3, the interpolation in energy between states at a given r_s is easily found. Figure 6 is an

example, showing the cusps at $r_s = 0$. Of course, this interpolation ignores the hierarchy states completely.

REFERENCES

- [1] G. Vignale and Mark Rasolt, Phys. Rev. Lett. **59**, 2360 (1987).
- [2] G. Vignale and Mark Rasolt, Phys. Rev. B **37**, 10685 (1988).
- [3] G. Vignale, Phys. Rev. B **47**, 10105 (1993).
- [4] M. Ferconi and G. Vignale, Phys. Rev. B **50**, 14772 (1994).
- [5] P. Skudlarski and G. Vignale, Phys. Rev. B **48**, 8547 (1993).
- [6] Mark Rasolt and F. Perrot, Phys. Rev. Lett. **69**, 2563 (1992).
- [7] B. Tanatar and D. M. Ceperley, Phys. Rev. B **39**, 5005 (1989).
- [8] D. Ceperley, Phys. Rev. B **18** 3126 (1978).
- [9] D. Levesque, J. J. Weis, and A. H. MacDonald, Phys. Rev. B **30**, 1056 (1984).
- [10] F. D. M. Haldane, Phys. Rev. Lett. **51**, 605 (1983).
- [11] G. Fano, F. Ortolani, and E. Colombo, Phys. Rev. B **34**, 2670 (1986).
- [12] T. T. Wu and Chen Ning Yang, Nucl. Phys. B **107**, 365 (1976).
- [13] S. Fahy, X. W. Wang, and Steven G. Louie, Phys. Rev. B **42**, 3503 (1990).
- [14] D. Ceperley, G. V. Chester, and M. H. Kalos, Phys. Rev. B **16**, 3081 (1977).
- [15] A. H. Macdonald and S. M. Girvin, Phys. Rev. B **33**, 4414 (1986).
- [16] J.K. Jain, Phys. Rev. Lett. **63** (1989) 199; Phys. Rev. B **40**, 8079 (1989); *ibid.* **41**, 7653 (1990).
- [17] N.E. Bonesteel, Phys. Rev. B **51**, 9917 (1995).
- [18] personal communication, Jon Leech (leech@cs.unc.edu) (1989).
- [19] K. Binder,

Ed., *Monte Carlo methods in statistical physics*, 2nd Ed. (Springer-Verlag, New York, 1986).

[20] F. C. Zhang and S. Das Sarma, *Phys. Rev. B* **33**, 2903 (1986).

[21] W. H. Press *et al*, *Numerical Recipes in C: The Art of Scientific Computing*, 2nd Ed., (Cambridge University Press, New York, 1992).

FIGURES

FIG. 1. Pseudopotential $u(r)$ for various α with cusp condition satisfied (13) and not satisfied (12). The solid lines correspond to (13) and the dashed lines to (12).

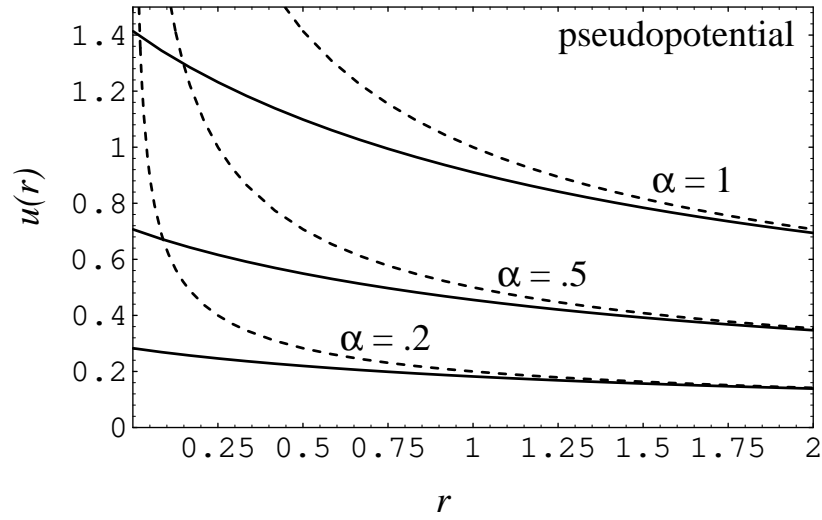


FIG. 2. Subdivision of a triangular octahedron face into smaller triangles as part of the initialization procedure for the Monte Carlo code.

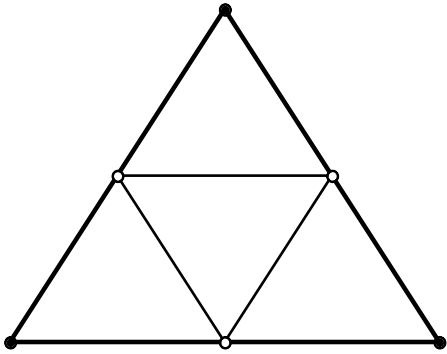


FIG. 3. Correlation energy $\bar{\epsilon}_{xc}$ as a function of r_s at various filling factors ν . Landau-level mixing is more pronounced at higher filling factors, as expected.

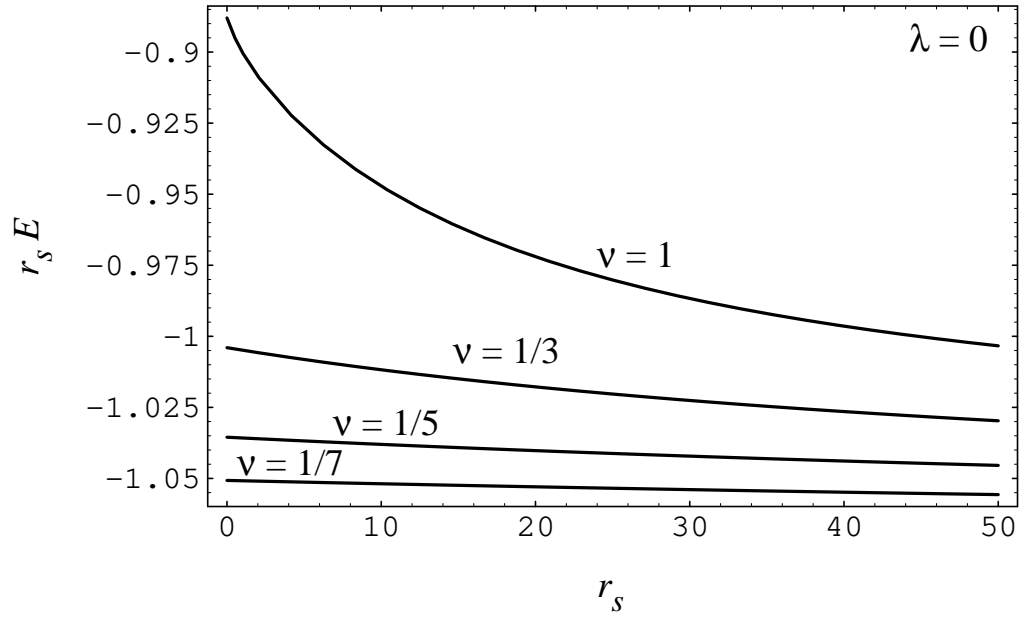


FIG. 4. Quasiparticle gap Δ_{eh} at $\nu = 1/3$ as a function of r_s .

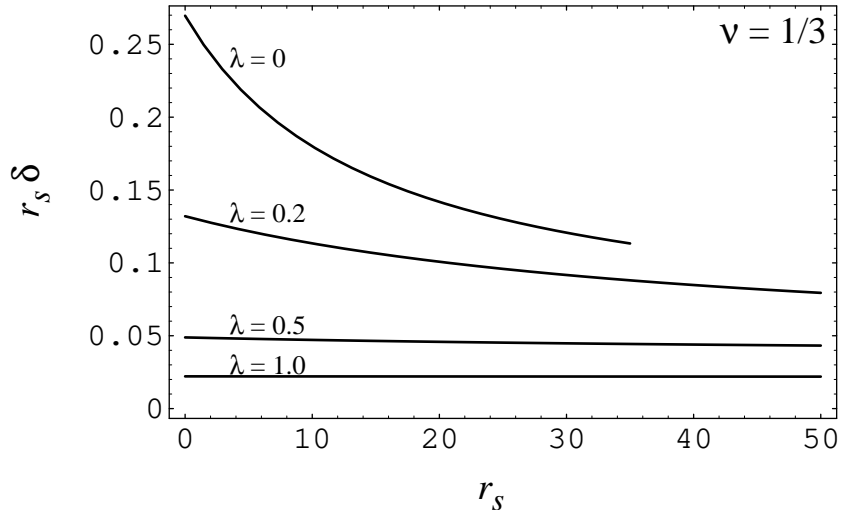


FIG. 5. Quasiparticle gap Δ_{eh} at $\nu = 1/7$ as a function of r_s . Landau-level mixing continues to have an effect here, although the effect on total energy is miniscule.

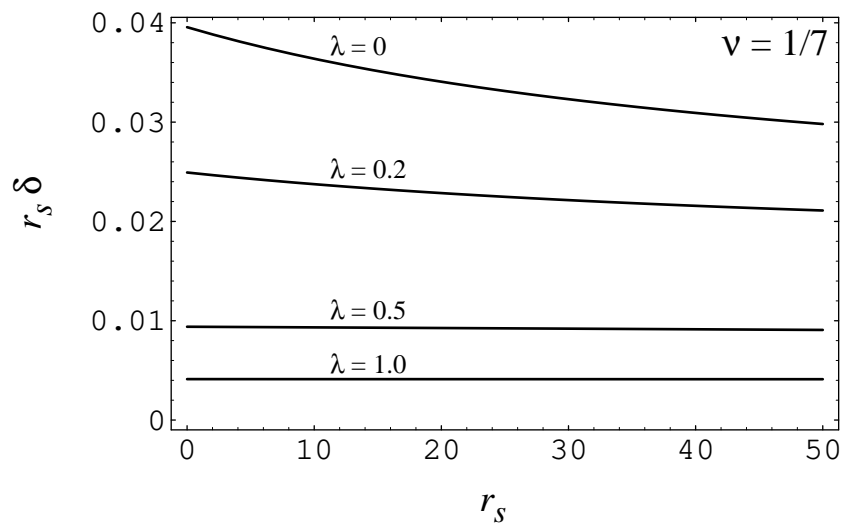
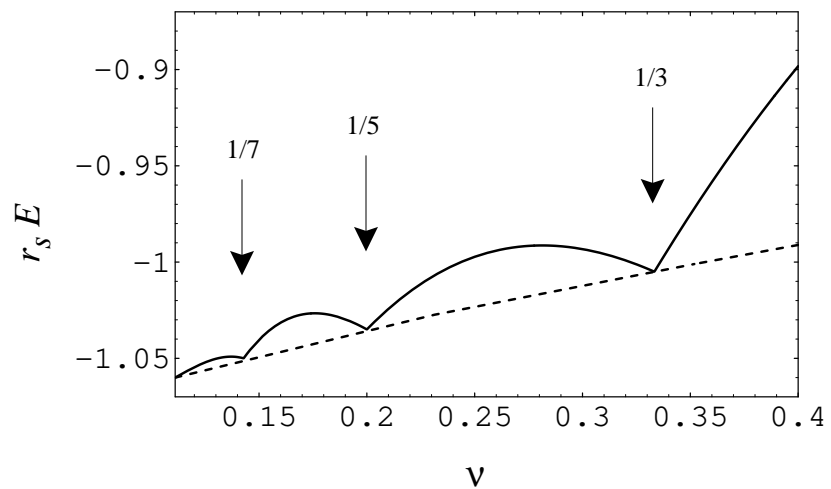


FIG. 6. Spline interpolation between energies at $\nu = 1/3, 1/5,$ and $1/7$, showing cusps in energy at principal FQHE states. Here $r_s = 0$. The dotted line is a smooth cubic spline interpolation between FQHE states.



TABLES

TABLE I. Parameters for a (2,2) rational function fit to the correlation energy $\bar{\epsilon}_{xc}$ for the Coulomb interaction ($\lambda = 0$).

ν	a_0	a_1	b_1	$a_2 \times 10^3$	$b_2 \times 10^3$
2	-0.864(2)	-0.3883	0.4221	-19.85	18.97
1	-0.888(2)	-0.7518	0.8281	-41.28	39.52
1/3	-1.004(1)	-0.01561	0.01466		
1/5	-1.0355(8)	-0.007768	0.007241		
1/7	-1.0507(5)	-0.004958	0.004602		

TABLE II. Parameters for a (2,2) rational function fit to the correlation energy $\bar{\epsilon}_{xc}$ with $\lambda = 0.2$.

ν	a_0	a_1	b_1	$a_2 \times 10^3$	$b_2 \times 10^3$
2	-1.7220(1)	-0.2843	0.4221	-4.081	2.327
1	-1.7322(1)	-0.093231	0.053603	-0.21638	0.12166
1/3	-1.75085(5)	-0.00677			
1/5	-1.75623(5)	-8.2×10^{-6}			
1/7	-1.75891(5)	-3.9×10^{-6}			

TABLE III. Parameters for a (1,1) rational function fit to the correlation energy $\bar{\epsilon}_{xc}$ with $\lambda = 0.5$.

ν	a_0	a_1	b_1
2	-3.22068(1)	-0.0460183	0.0142792
1	-3.22281(1)	-4.458×10^{-6}	
1/3	-3.22492(1)	-2.133×10^{-7}	
1/5	-3.22540(1)	-5.4×10^{-8}	
1/7	-3.22562(1)	-2.0×10^{-8}	

TABLE IV. Parameters for a linear fit to the correlation energy $\bar{\epsilon}_{xc}$ with $\lambda = 1.0$.

ν	a_0	a_1
2	-4.81968(1)	-6.26×10^{-7}
1	-4.82005(1)	-8.45×10^{-8}
1/3	-4.82034(1)	-2.73×10^{-9}
1/5	-4.82040(1)	-6.5×10^{-10}
1/7	-4.82042(1)	-2.3×10^{-10}

TABLE V. Parameters for a (1,1) rational function fit to the gap energy Δ_{eh} for the Coulomb interaction ($\lambda = 0.0$).

ν	a_0	a_1	b_1
2	0.43(4)	0.047	0.321
1	0.80(8)	0.0239	0.176
1/3	0.27(3)	0.00317	0.0674
1/5	0.076(8)	-6.15×10^{-6}	0.0107
1/7	0.040(5)	3.62×10^{-4}	0.0187

TABLE VI. Parameters for a (1,1) rational function fit to the gap energy Δ_{eh} with $\lambda = 0.2$.

ν	a_0	a_1	b_1
2	0.32(5)	0.0213	0.164
1	0.56(8)	0.00735	0.0711
1/3	0.13(2)	0.000847	0.0239
1/5	0.046(7)	-0.000177	0.0
1/7	0.025(4)	0.000251	0.0155

TABLE VII. Parameters for a (1,1) rational function fit to the gap energy Δ_{eh} with $\lambda = 0.5$.

ν	a_0	a_1	b_1
2	0.20(4)	0.00568	0.0472
1	0.30(6)	0.00233	0.0185
1/3	0.049(9)	0.000545	0.0152
1/5	0.018(4)	-1.12×10^{-5}	0.0
1/7	0.009(2)	-6043×10^{-6}	0.0

TABLE VIII. Parameters for a (1,1) rational function fit to the gap energy Δ_{eh} with $\lambda = 1.0$.

ν	a_0	a_1	b_1
2	0.14(3)	0.00248	0.0196
1	0.17(4)	0.00118	0.00819
1/3	0.022(5)	-3.7×10^{-6}	0.0
1/5	0.008(2)	-4.4×10^{-7}	0.0
1/7	0.004(1)	-1.9×10^{-7}	0.0